

The Proteomic Signature of *Aspergillus fumigatus* During Early Development

Steven E. Cagas¹, Mohit Raja Jain², Hong Li² and David S. Perlin^{1*}

¹Public Health Research Institute and ²Center for Advanced Proteomics Research

New Jersey Medical School - University of Medicine and Dentistry of New Jersey.

Newark, NJ 07103.

*To whom correspondence should be addressed

David S. Perlin, Ph.D.

Public Health Research Institute

UMDNJ-New Jersey Medical School

225 Warren Street, Newark, NJ 07103 USA

973 854-3200 (voice); 973 854-3101 (fax); Email: perlinds@umdnj.edu

Running Title: Early Development *A. fumigatus* proteome profile

Summary

Aspergillus fumigatus is a saprophytic fungus that causes a range of diseases in humans including invasive aspergillosis. All forms of disease begin with the inhalation of conidia which germinate and develop. Four stages of early development were evaluated using the gel free system of isobaric tagging for relative and absolute quantitation (iTRAQ) to determine the full proteomic profile of the pathogen. A total of 461 proteins were identified at 0, 4, 8, and 16 hours and fold changes for each were established. Ten proteins including the hydrophobin rodlet protein RodA and a protein involved in melanin synthesis Abr2 were found to decrease relative to conidia. To generate a more comprehensive view of early development, a whole genome microarray analysis was performed comparing conidia to 8 and 16 hours of growth. A total of 1871 genes were found to change significantly at 8 hours with 1001 genes up-regulated and 870 down-regulated. At 16 hours, 1235 genes changed significantly with 855 up-regulated and 380 down-regulated. When a comparison between the proteomics and microarray data was performed at 8 hours, a total of 22 proteins with significant changes also had corresponding genes that changed significantly. When the same comparison was performed at 16 hours, 12 protein/gene combinations were found. This study, the most comprehensive to date, provides insights into early pathways activated during growth and development of *A. fumigatus*. It reveals a pathogen that is gearing up for rapid growth by building translation machinery, generating ATP, and is very much committed to aerobic metabolism.

Introduction

Aspergillus fumigatus is a saprophytic mold that thrives in the soil on organic debris. It sporulates readily with conidiophores producing multitudes of conidia [1]. This microbe can also cause disease in humans ranging from invasive aspergillosis in hosts with a compromised immune system to allergic bronchopulmonary aspergillosis (ABPA) in hosts with an overactive immune response [2,3]. All manifestations of disease begin with the inhalation of conidia or hyphal elements. In patients with an intact immune system, the conidia are usually cleared by macrophages and neutrophils in both the nose and lungs along with mucocilliary mechanisms [2,4]. When the immune system is compromised by neutropenia, solid organ transplant, advanced AIDS, or several other diseases, the conidia can germinate and invade the lung or surrounding tissue [5]. Conidial germination is a process which can be divided into four stages: (i) breaking of spore dormancy; (ii) isotropic swelling; (iii) establishment of cell polarity; and (iv) formation of a germ tube and maintenance of polar growth [6,7,8]. Identifying proteins involved in this process can lead to potential biomarkers of active *A. fumigatus* infection and could also be used to design and evaluate potential new therapeutic targets *in vitro*, or examine the efficacy of current treatments in experimental models. Early initiation of antifungal therapy is critical and leads to improved clinical outcomes [1]. Conidia have been the focus of much of the research in development thus far due to the fact that they are the first structure that the immune system encounters during an infection [9]. Conidia have at least 2 characteristics that allow them to evade the host immune system: melanin and the outer rodlet layer. The main pigment of *Aspergillus fumigatus*, melanin, is produced by a complex of six genes and has also been shown to have a role

Early Development *A. fumigatus* proteome profile

in conidia cell wall integrity [10,11]. Colorless mutants of *A. fumigatus* have also been shown to be less virulent and more easily detectable by the immune system [12]. The outer rodlet layer, encoded by *rodA* and to a lesser extent *rodB*, functions in masking the conidia from the immune system as well as in cell wall integrity [13,14,15]. Mutations have been generated in *A. fumigatus rodA* which yields no rodlet layer and the spores are readily detected by the immune system [13].

The first positive identification of proteins from conidia yielded 26 proteins [9]. Sixteen allergens were also identified from 2D gels using tandem mass spectroscopy which were then tested against patient sera [16]. More recently genomic approaches such as real time reverse transcription PCR and macroarray analyses were used to track specific genes during infection. Real time RT-PCR was used to evaluate 12 genes of *A. fumigatus* from infected mouse lung samples [17], while a more comprehensive macroarray study of more than 3,000 genes was conducted by Lamarre et al. [8]. A recent study used 2D gel electrophoresis to map 449 different proteins present in conidia and 2D differential in-gel electrophoresis (DIGE) to compare the proteins present in resting conidia to those present in mycelia [18]. 2D gel electrophoresis has been the standard approach for the past 20 years, but it has the limitations of profiling only the most highly abundant proteins and difficulty quantifying them [19]. The gel free system of isobaric tagging for relative and absolute quantitation (iTRAQ) has the ability to simultaneously analyze 8 samples while identifying hundreds of proteins with quantitation for each one relative to any other sample [20,21]. To assess the proteins that are both turned on and turned off during the germination process, the iTRAQ system was used to analyze samples kinetically from conidia to young hyphae. In a

Early Development *A. fumigatus* proteome profile

complementary approach, a whole genome microarray was used to assess the gene expression profile of germinating and developing conidia. These data were validated against previous research in our lab [22] comparing these proteins to those that are increasing and decreasing in response to the echinocandin antifungal drug caspofungin. This is the most comprehensive study to date, simultaneously tracking 461 proteins with quantification over 4 time points as well as using the whole genome microarray to give gene information at 2 different time points for over 9,000 open reading frames. This data is critical for the identification and evaluation of new biomarkers of active *A. fumigatus* infection and possible new antifungal targets.

Materials and Methods

Strains, Media, and Culture Conditions

Aspergillus fumigatus strain R21 (H11-20)[23], a clinical isolate, was grown at 37°C on potato dextrose agar (PDA, Becton Dickinson, Sparks, Maryland) for at least 72 hours to generate conidia. Spores were harvested using sterile dH₂O containing 0.1% Tween (Sigma Aldrich, St. Louis, MO) and counted using a hemocytometer. Cultures were inoculated at a concentration of $1 \cdot 10^5$ conidia/ml in YPD broth (2% yeast extract, 4% Bacto peptone, 4% dextrose) for 4, 8, and 16 hours with shaking at 225 rpm. At 4h and 8h, the cultures were centrifuged at 10,000 xg for 15 minutes and the pellet of cellular material was collected. The T₁₆ material was recovered by filtration through Miracloth (CalBiochem, La Jolla, CA) after the allotted time. All material was washed twice with cold sterile dH₂O before storage at -80°C. All material was generated in biological duplicate unless otherwise indicated.

Microarray Analysis

(i) Isolation of RNA from *Aspergillus fumigatus*

Strains were grown for 8 or 16 hours in triplicate, as above, and all samples were lysed by crushing in a mortar and pestle under liquid nitrogen for a minimum of 5 minutes. A total of $2.1 \cdot 10^{11}$ conidia were used to generate a sufficient amount of RNA to use for microarray analysis. The finely ground powder was then processed using the RNeasy Maxi Kit (Qiagen Inc., Valencia, CA). The ground mycelia was used as the initial sample and resuspended in the kit supplied Buffer RLT. The rest of the protocol was as per the manufacturer's instructions. RNA was DNase treated at 1U/5ng RNA at 37°C for 15 minutes using Turbo DNase (Ambion, Austin, TX) followed by heat inactivation of the enzyme at 75°C for 5 minutes. Following DNase treatment the RNA was measured for quantity and purity using RNA Nano Chips and the Agilent 2100 Bioanalyzer. (Agilent Technologies, Waldbronn, Germany).

(ii) Labeling, Pre-Hybridization, and Hybridization of DNA Slides

A. fumigatus total RNA (2µg) was labeled using protocols outlined by The Institute for Genomic Research (TIGR) SOP #M007 (<http://pfgrc.jcvi.org/index.php/microarray/protocols.html>). All slides were whole genome *A. fumigatus* DNA version 3 (J. Craig Venter Institute, Rockville, MD). SuperScript III (Invitrogen, Carlsbad, CA) was used instead of PowerScript RT in the labeling reactions as PowerScript RT has been discontinued. The hybridization of the labeled probes was performed as per SOP#M008. The coverslips used were thick LifterSlip coverslips (Erie

Early Development *A. fumigatus* proteome profile

Scientific Company, Portsmouth, NH) and hybridization chamber with an increased depth (Corning, Lowell, MA).

(iii) Image Acquisition and Data Analysis

All slides were scanned using an Axon Instruments model 4000B (Molecular Devices, Sunnydale, CA) with each channel being scanned individually. All scans used a 10 μ m resolution and were converted into a resolution of 16 bits/pixel. All scanned images were then analyzed using the GenePix Pro 6.1 software. After global normalization in GenePix Pro, SAM analysis was performed on all data using TM4 software [24]. The remaining data was then filtered by taking the mean of all data points for that spot (3 replicates with dye swap) and any gene with an expression value >2 was considered significant.

(iv) Biological Theme Determinations

Identification of biological themes that were over-represented was determined using the Expression Analysis Systematic Explorer (EASE) program embedded within the TIGR TM4 software package [25] (<http://www.tm4.org>). The number of genes in each Gene Ontology category for Biological Process, Cellular component and Molecular Function were compared to the whole genome dataset for overrepresented categories and only categories with Fisher's exact test p -values <0.05 were included based on previous research [26].

Protein extraction and iTRAQ labeling

Early Development *A. fumigatus* proteome profile

Conidia (10^9), 4 and 8 h cells were lysed by crushing for 5 minutes in a mortar and pestle under liquid nitrogen. This material was then resuspended in lysis buffer (50mM HEPES, 20% Glycerol, 1mM EDTA, 1mM PMSF, and 1mM DTT) for further processing. The 16 h material was resuspended in lysis buffer and lysed by passing through a French Press at 20,000 psi 5 times. All samples were then spun at 5,000 xg to remove cells that were not lysed. The remaining supernatant was then used for downstream protein processing. After acetone precipitation, protein pellets were solubilized in digestion buffer (500 mM TEAB, 1.0 % Igepal CA630, 1.0 % Triton X-100, Sigma protease inhibitor cocktail) and disrupted by sonication in a 4°C water bath. The sample was adjusted to pH 8.0 with 1.0 M TEAB. One hundred µg of protein from each sample was used for this analysis. After reduction with TCEP and alkylation with MMTS, tryptic digestion was performed by addition of 5 µg of trypsin (Promega Corporation, Madison, WI) to each of the eight samples at 37 °C for 14 h. An aliquot of the sample was run on an SDS-PAGE gel and stained with SYPRO ruby to test for complete tryptic digestion. Peptides derived from conidia were labeled with iTRAQ tags 113 and 114, with the 4 hour samples being labeled with 115 and 116, 8 hour samples labeled with 117 and 118, and the 16 hour samples labeled with 119 and 121 as per manufacturer's instructions. The labeled samples were then mixed together and fractionated via two dimensional liquid chromatography as previously described [27]. The HPLC eluent was mixed with matrix solution (7 mg/ml alpha-cyano-4-hydroxycinnamic acid in 50% ACN, 5 mM of ammonium monobasic phosphate) and the internal mass calibrants, (50 fmol/µl each of [Glu1]-Fibrinopeptide B and adrenocorticotrophic hormone fragment 18-39) through a 30 nl mixing tee before directly spotting onto 1,650 well MALDI plates.

MALDI-TOF/TOF tandem MS analysis

The peptides were analyzed on an ABI 4800 Plus MALDI TOF/TOF Analyzer with 4000 series explorer software (version 3.5.3) in a data-dependent fashion using a job-wide interpretation method. MS spectra (m/z 800–3,600) were acquired in positive ion reflection mode with internal mass calibration. A total of 1,000 laser shots were accumulated for each spot. A maximum of fifteen most intense ions (S/N ≥ 50) per spot were selected for succeeding MS/MS analysis in 2.0 keV mode using air as a CID gas at pressure of 1×10^{-6} Torr. A total of 4,000 laser shots were accumulated for each spectrum.

Protein database search and bioinformatics

TS2Mascot Version 0.0.90 (Matrix Science Inc., Boston, MA) was used to generate a peak list as mascot generic file (MGF) from tandem MS using parameters: mass range from 20-60 Dalton below precursor, S/N ratio 10. MGF was submitted for automated search using local Mascot server (version 2.3) against Reverse Concatenated FASTA Database of *Aspergillus fumigatus* protein database (9,630 entries, curated from Uniprot Release 2010_12 (downloaded from <ftp://ftp.ebi.ac.uk/pub/databases/uniprot/knowledgebase>) on November 30, 2010). The following parameters were used; iTRAQ 8plex (K), iTRAQ 8plex (N-terminal) and methylthio (C) as fixed modifications; iTRAQ 8plex (Y) and Oxidation (M) as variable modifications; trypsin as enzyme with maximum one missed cleavage allowed; monoisotopic, peptide tolerance 50 ppm; MS/MS tolerance 0.3 Da. Scaffold (version Scaffold_2_06_01, Proteome Software Inc., Portland, OR) was used to validate MS/MS

Early Development *A. fumigatus* proteome profile

based peptide and protein identifications. Peptide identifications were accepted if they could be established at greater than 95.0% probability as specified by the Peptide Prophet algorithm [28]. Protein identifications were accepted if they could be established at greater than 99.0% probability and contained at least 2 identified peptides. False discovery rate was calculated and was 5.3% at the peptide level and 0.0% at the protein level [29]. Protein probabilities were assigned by the Protein Prophet algorithm [30]. Proteins that contained similar peptides and could not be differentiated based on MS/MS analysis alone were grouped to satisfy the principles of parsimony. Peptides were quantitated using the centroided reporter ion peak intensity. Intra-sample channels were normalized based on the median ratio for each channel across all proteins. Multiple isobaric tag samples were normalized by comparing the median protein ratios for the reference channel. Protein quantitative values were derived from only uniquely assigned peptides. The minimum quantitative value for each spectrum was calculated as 5.0% percent of the highest peak. Protein quantitative ratios were calculated as the median of all peptide ratios. Standard deviations were calculated as the interquartile range around the median. Quantitative ratios were Log_2 normalized for final quantitative testing. For each identified protein, associated gene ontology terms were automatically fetched from NCBI by Scaffold software and plotted with respect to enrichment.

Results

Proteomic Signature During Germination and Growth

Upon addition of conidia to rich media, they begin uptake of water, swell at 4 hours, and establish a germ tube at 8 hours; full hyphal branching is evident at 16 hours (Figure 1).

Early Development *A. fumigatus* proteome profile

To establish the proteomic changes at these critical stages, the system of gel-free isobaric tagging for relative and absolute quantitation (iTRAQ) was used. The iTRAQ system was able to identify a total of 461 proteins with 231 of these being identified with high confidence (2 different peptides derived from a given protein with a confidence of 95% and protein identification of at least 99%). Only high confidence proteins were used for downstream analysis.

A total of 10 proteins were shown to decrease at least 2-fold at 4, 8, and 16 hours. These proteins include *abr2*, the hydrophobin *rodA*, heat shock protein *hsp30/hsp42*, the copper-zinc superoxide dismutase *sodC*, as well as a putative carboxylase and a putative protein (Table 1). The *abr2* protein decreased by 10.2 fold at 4 hours, 25.2 fold at 8 hours and 24.3 fold at 16 hours compared with T0. A total of 12 proteins decreased at least 2-fold in 2 of the 3 time points tested. These include a putative decarboxylase which decreased 2.5-fold at 4 hours and 6.8-fold at 8 hours, transaldolase which decreased 2.6-fold at T4 and 2.7 fold at T8, adenosine kinase which decreased 2.3-fold at T8 and 2.0-fold at T16, *GatA* which decreased 2.7-fold at T8 and 3.8-fold at T16 along with 1 putative uncharacterized protein (Table 1). Another subset of 24 proteins decreased 2-fold or greater at only a single time point. These include the nucleolin protein *Nsr1* which was not significantly changed at 4 or 8 hours compared to conidia, but showed at 3.0-fold decrease at T16. The same pattern was seen for *eEF-3* with a decrease of 2.2-fold, ABC transporter *Arb1* with a 2.2-fold decrease, and the RNA helicase *ded1*. Other proteins showed a significant decrease at T8 including glucose 6 phosphate isomerase at 2.3-fold decreasing, catalase-peroxidase *katG* decreasing 2.9-fold, protein disulfide isomerase *pdi1* at 3.0-fold decreasing, and the actin cytoskeleton

Early Development *A. fumigatus* proteome profile

protein Vip1 decreasing 4.0-fold at T8. There was also a putative uncharacterized protein (AFUA_6G10450) that showed a decrease of 3.7-fold at the T8 time point (Table 1). No proteins in the current study showed a decrease at only the 4 hour time point.

A total of 24 proteins showed an increase of 2-fold or greater over the time course (Table 1). However, only 1 protein showed an increase of greater than 2-fold at all 3 time points tested, the RAN-specific GTPase activating protein 1. This protein increased 2.1-fold at 4 hours, 2.1-fold at 8 hours, and 2.5-fold at 16 hours.

Some proteins such as *fpr4* showed a biphasic increase of 2.1-fold at T8 and a decrease of 2.4-fold at T16. Other proteins such as the phosphoenolpyruvate carboxykinase *AcuF* decreased 2.3-fold at T8 with an increase of 2.4-fold at T16. One putative uncharacterized protein (AFUA_5G14680) showed a similar pattern with a decrease of 2.9-fold at T8 and an increase of 2.1-fold at T16 (Table 1).

Genomic Changes

Microarray analysis was performed in parallel to test differences in gene expression between cells at T0 vs. T8 as well as T0 vs. T16. A total of 1871 genes were found to have significant changes in expression (2.0-fold or greater) at 8 hours compared to conidia (Supplementary Table S1). Of these genes, 1001 were up-regulated and 870 were down-regulated. The gene with the most dramatic decrease was the ComA domain protein with a decrease of 153.7 fold. Three other genes including a monosaccharide transporter, a hypothetical protein (AFUA_6G12000) and an alcohol dehydrogenase all had decreases in fold change greater than 100 (Table 2 and Supplementary Table S1). The largest changes in up-regulation were seen in HEX1

Early Development *A. fumigatus* proteome profile

with a fold change of 34.2 and c-4 methyl sterol oxidase with an increase of 29.6-fold (Table 2 and Supplementary Table S1). Gene Ontology information indicated that the favored biological processes for the 870 genes that decreased included fatty acid β -oxidation, fatty acid catabolism, autophagy, and the hyperosmotic response. Their localization is likely to be in the peroxisomal matrix or membrane and the molecular function is involved in zinc ion binding, RNA polymerase II transcription factor activity, or two component sensor activity (Supplementary Table S2). Of the 1001 genes that increased the most dominant biological process induced is translation involving both the large and small cytosolic ribosomal subunits (Supplementary Table S3).

The number of genes with significant changes at 16 hours was 1235 with 855 increasing and 380 decreasing. The gene with the largest decrease between the two time points was isocitrate lyase with a decrease of 172.8-fold. This was followed by a hypothetical protein (AFUA_1G01490) with a decrease of 158.5-fold, cytochrome P450 monooxygenase with a decrease of 150.8-fold, and the same monosaccharide transporter as T8 with a decrease of 142.0-fold. A total of 8 genes had decreased fold changes greater than 100 (Table 2 and Supplementary Table S4). The largest change was seen in endochitinase with an increase of 115.3-fold compared with T0. Other genes such as an MFS monosaccharide transporter had an increase in gene expression of 98.5-fold, secreted dipeptidyl peptidase had an increase of 93.4-fold and the allergen AspF4 had an increase of 89.2-fold (Table 2 and Supplementary Table S4). The gene ontology information obtained for the 380 decreasing genes indicates that the favored biological process is again fatty acid β -oxidation as well as N-acetylglucosamine catabolism. The cellular component for these processes is the peroxisome and the

Early Development *A. fumigatus* proteome profile

peroxisomal matrix with the favored molecular function being electron transporter activity (Supplementary Table S5). For the 855 increasing genes, the most highly favored biological process is still translation along with ATP synthesis coupled proton transport as well as mitochondrial electron transport. These indicate a large push towards ATP generation through the electron transport chain (Supplementary Table S6).

Proteomic/Genomic Comparison

A total of 231 proteins were identified with high confidence using the gel-free system of iTRAQ at 4 time points: 0 hours, 4 hours, 8 hours, and 16 hours. To compare the changes in the proteome with changes in the genome, microarray analysis was evaluated at 8 and 16 hours of growth relative to T0. A total of 1871 genes changed 2-fold or more at 8 hours and 1235 changed 2-fold or more at 16 hours. At the 8 hour time point, 57 combinations of genes and proteins with significant changes were found, but only 22 had changes in the same direction (Table 3 and Supplementary Table S7). These include heat shock proteins Hsp30/Hsp42 with a decrease in protein level by 28.6-fold and a decrease in gene level by 25.5-fold. Glutamine synthetase had a small change in protein level (down 3.5-fold) but a large change in gene expression level (down 20.6 fold). Of the 17 proteins that showed significant increases at 8 hours, 16 were also identified as significantly increasing by microarray (Table 3 and Supplementary Table S7); 12 of these proteins were ribosomal proteins. The largest change seen by proteomics in these proteins was an increase of 2.6-fold in the 40S ribosomal protein S15, but the largest change by microarray was 15.3-fold in the nascent polypeptide-associated complex subunit alpha. Some protein/gene

Early Development *A. fumigatus* proteome profile

combinations have values that differ vastly such as flavohemoprotein which had a decrease in protein level of 3.3-fold but an increase in gene level of 14.2-fold. The same pattern was observed with the pyruvate peroxiredoxin pmp20, which has a protein decrease of 2.2-fold but a gene increase of 9.3-fold. Other proteins that showed significant changes in expressed protein such as abr2, Cu-Zn superoxide dismutase, rodA, and the putative uncharacterized protein (AFUA_8G00630), all with decreases of greater than 10-fold, were not detected by microarray analysis at the time points evaluated.

At the 16 hour time point, 18 protein/gene combinations were observed in which both proteins and genes changed 2-fold or greater (Table 4 and Supplementary Table S8). Of these, 12 combinations showed a given protein and gene changing in the same direction (6 decreasing and 6 increasing.) None of the 9 proteins with the largest decreases by proteomics were identified in the microarray analysis suggesting a rapid turnover of mRNA. Decreasing proteins with a genomic counterpart included the nucleolin protein Nsr1 with a protein decrease of 3.0-fold and a gene decrease of 2.8-fold, ABC transporter Arb1 with protein fold decrease of 2.2 and gene decrease of 4.7-fold, Asn2 for asparagine synthetase with a protein decrease of 2.1-fold and gene decrease of 2.2-fold, and the RNA helicase ded1 with protein fold decrease of 2.1 and gene decrease of 8.4-fold. A similar pattern of larger changes in gene expression than changes in relative protein level was also seen at 16 hours. The translation elongation factor eEF-3 showed a gene change 5.7 times that of the protein change (12.5 for the gene and 2.2 for the protein) while the glutamine synthetase showed a gene change 7.2 times that of the protein change (20.9 fold for the gene vs. 2.9 fold for the protein). Of

Early Development *A. fumigatus* proteome profile

the 6 proteins that increased, 3 were putative uncharacterized proteins (Table 4 and Supplementary Table S8). AFUA_5G14680 increased 2.1-fold in the protein and 24.3-fold in the gene; AFUA_8G05600 had a 2.5-fold protein expression increase with a 32.9-fold gene expression increase, and AFUA_3G06460 had a 2.5-fold increase in protein with an 8.9-fold increase in gene expression. Other combinations included a 57 kDa immunogenic protein (AFUA_4G12450), tropomyosin, and the same GTPase activating protein as T8. The protein with the largest change was cytochrome c with an increase of 2.6-fold, but the gene was not detected above baseline in the final analysis.

Discussion

The *Aspergillus fumigatus* proteome is complex and highly dynamic during the early stages of development following conidial germination. A classical 2D gel approach to evaluate changes in the proteome during early development suffers from an inherent lack of sensitivity. This issue was seen with the mapping of the proteome of conidia by Teutschbein et al. [18] in which one 2D gel was unable to resolve all protein spots. To increase the relative resolving power this group used 2D gels with narrow pI ranges, but this led to many spots being identified multiple times. To circumvent these problems and improve resolution, a gel-free system of iTRAQ was used to identify 461 proteins, more than Teutschbein et al., along with quantitative measurements of the protein amount over several time points, which is unique to this study. The time points chosen for this study were selected because they are at critical early development stages for the cell including the swelling of conidia, the formation of a germ tube and a culture that has become more mature. These developmental stages elicit protein signatures that portend early *A. fumigatus* infection. At the earliest time point, T4, 15 proteins showed

Early Development *A. fumigatus* proteome profile

a decrease of 2-fold or greater indicating that these proteins are either present in the conidium itself or are transcribed and translated at a very early time point. Of the 40 most abundant proteins in conidia by 2D analysis, 30 were also present in our analysis and 24 were high confidence proteins (2 unique peptides of 95% confidence, protein identification at least 99%). Some proteins are expected to decrease and therefore serve as a validation of the approach including RodA which forms the rodlet layer on the surface of conidia [13] and decreased by 10.6-fold. The *abr2* gene encoding the final enzyme in the melanin biosynthetic pathway decreased by 10.2-fold at 4 hours and continued to decrease to over 25-fold at 8 hours and 24.3 fold at 16 hours. The proteins that increase at T4, as well as the other time points, suggest a large increase in ribosomal genes consistent with the increases in translation necessary for growth. These proteins and their pathways, including cytochrome C, the 57kDa immunogenic protein, as well as members of the TCA cycle, are potential targets for new antifungals or possible biomarkers of active infection.

Previously it was reported that a total of 63 proteins decreased in mycelia vs. conidia while 38 increased [18]. Consistent with these results, we found 65.7% (25/38) of the reported proteins that increased; yet only 25.4% (16/63) of decreasing proteins. Of the proteins that were identified, the trend behavior is consistent although the absolute fold changes observed are different, as expected. Certain signature proteins such as RodAp showed a similar pattern decreasing by 10.9-fold in this study and 27.3-fold and 21.5-fold previously [18]. Some proteins showed a poor correlation such as the NAD-dependant formate dehydrogenase *AciA/Fdh*, which remained consistent in our time course while a large decrease of 44.4, 9.5, and 4.5-fold was observed in the 2D study

Early Development *A. fumigatus* proteome profile

[18]. This may reflect the nutritional source of the culture. The current study had all cultures grown in a rich YPD medium whereas Teutschbein et al. [18] grew their cultures in a more defined AMM supplemented with 50mM glucose. Of the 41 common proteins found between the two studies, over 50% (22) changes were in the same direction. Overall these data suggest that both gel free and gel based systems yield important information about expressed proteins during growth and development.

To provide a more comprehensive view of the early development of *A. fumigatus* a whole genome microarray analysis was performed to assess the relationship between gene expression and protein abundance. This combined analysis is unique to this study in *Aspergillus fumigatus* development. Analysis of the genomic and proteomic profiles reflects a dynamic cell undergoing a rapid transfer toward aerobic growth and development. The T8 microarray data and the iTRAQ agree inasmuch as the biological process of translation shows the most significant increase and 70.5% (12/17) of the proteins increasing the most are ribosomal. The microarray data of the genes that are down-regulated also shows that the synthesis of fatty acids is a critical early process at this time suggesting that they may be possible biomarker or antifungal targets. At T16, similar trends are shown with the data indicating that translation is still very active as is fatty acid synthesis. N-acetylglucosamine synthesis is also up-regulated, which is consistent with chitin being integrated into the rapidly expanding cell wall for structural integrity. One previous study also looked at the changes in expression during the exit from dormancy of spores, and although a full microarray was not used many of the results are consistent with our data [8]. The study by Lamarre et al. [8] used time points earlier than those chosen in the current study (8 and 16 hours in the current

Early Development *A. fumigatus* proteome profile

study vs. 30, 60, and 90 minutes post inoculation in the previous study). In that study, an array of 3,000 genes was utilized compared to our full genome microarray with over 9,000 genes represented. It was reported that the processes of protein, amino acid, and protein complex synthesis as well as ribosome biogenesis are increasing consistent with our microarray indicating that translation is the favored biological process during early development.

Another process found to be up-regulated in the current study was that of aerobic respiration. The GO information at 8 hours demonstrated that 15 genes identified were involved in this process including 3 subunits of the cytochrome C oxidase complex along with mitochondrial large ribosomal proteins. This is in agreement with previous studies that demonstrate that the process of aerobic respiration is required for *A. fumigatus* growth [31]. This process was also shown to be up-regulated by microarray at 16 hours demonstrating that aerobic respiration is still active during mature cultures with 3 subunits of the cytochrome C oxidase family increasing by at least 7.6-fold. The ubiquinol-cytochrome C reductase complex also had 5 members increased at 16 hours.

Validation of Findings

As a way to help validate the proteomic findings in this study, we have compared recent proteomic findings from a study involving inhibition of cell growth with the echinocandin drug caspofungin [22]. When caspofungin is added to a culture of *A. fumigatus*, it acts as a fungistatic agent, only allowing the formation of “rosette structures” [22]. Therefore if a certain protein decreases in the presence of caspofungin and increases during normal development, the caspofungin data can serve as an

Early Development *A. fumigatus* proteome profile

indirect validation for the development data. When the data from this study was compared to the previous proteomic research performed by Cagas et al. [22], there was overlap in many of the proteins observed. Of the 461 total proteins in this study, 216 were identified in two iTRAQs that were run with a caspofungin sensitive and resistant strain in the presence and absence of the drug. Of the 231 high confidence proteins identified in this study, 137 proteins were found to be in common with the previous research. These 137 common proteins were analyzed for possible information on the efficacy of current caspofungin treatment. Proteins involved electron transport such as cytochrome c and the cytochrome c subunit Va and Vb decrease by 3.48, 2.00, and 1.52-fold respectively in the presence of caspofungin, but increase 2.56, 1.71, and 1.63-fold during normal development at 16 hours. This same pattern hold true for enzymes involved in glycolysis such as phosphoglycerate kinase which increase 1.66-fold at 16 hours and decreases 3.48-fold when exposed to caspofungin. The 57kDa immunogenic protein which increased 2.15- fold during development and decreased 1.62-fold after exposure to caspofungin is also believed to be involved in metabolism and amino acid biosynthesis [32].

Overall, the current study provides the most comprehensive proteomic and genomic signature of *Aspergillus fumigatus* during germination and early development, which contributes to the overall understanding of this human pathogen. The results discovered in this study can impact the fields of fungal development, antifungal drug discovery, biomarker assessment as well as *Aspergillus* pathogenesis. These processes may be used for the discovery and assessment of novel biomarkers of active infection, as well as possible new therapeutic targets. It also reveals a pathogen that is

Early Development *A. fumigatus* proteome profile

gearing up for rapid growth by building translation machinery, generating ATP, and is very much committed to aerobic metabolism.

Acknowledgments

This work was supported by NIH grant AI069397 to D.S.P. I would like to acknowledge Steven Park and Guillermo Garcia-Effron for their helpful discussions and suggestions and Yanan Zhao and Cristina Jimenez-Ortigosa for critical reading of the manuscript. I would also like to thank Dr. Natalie Fedorova for her assistance using the TMEV software.

References Cited

1. Latge JP (1999) *Aspergillus fumigatus* and aspergillosis. *Clinical Microbiology Reviews* 12: 310-+.
2. Denning DW (1998) Invasive aspergillosis. *Clin Infect Dis* 26: 781-803; quiz 804-785.
3. Marr KA, Patterson T, Denning D (2002) Aspergillosis. Pathogenesis, clinical manifestations, and therapy. *Infect Dis Clin North Am* 16: 875-894, vi.
4. Feldmesser M (2006) Role of neutrophils in invasive aspergillosis. *Infect Immun* 74: 6514-6516.
5. Segal BH (2009) Aspergillosis. *N Engl J Med* 360: 1870-1884.
6. Barhoom S, Sharon A (2004) cAMP regulation of "pathogenic" and "saprophytic" fungal spore germination. *Fungal Genet Biol* 41: 317-326.

Early Development *A. fumigatus* proteome profile

7. Harris SD, Momany M (2004) Polarity in filamentous fungi: moving beyond the yeast paradigm. *Fungal Genet Biol* 41: 391-400.
8. Lamarre C, Sokol S, Debeaupuis JP, Henry C, Lacroix C, et al. (2008) Transcriptomic analysis of the exit from dormancy of *Aspergillus fumigatus* conidia. *BMC Genomics* 9: 417.
9. Asif AR, Oellerich M, Amstrong VW, Riemenschneider B, Monod M, et al. (2006) Proteome of conidial surface associated proteins of *Aspergillus fumigatus* reflecting potential vaccine candidates and allergens. *J Proteome Res* 5: 954-962.
10. Chai LY, Netea MG, Sugui J, Vonk AG, van de Sande WW, et al. (2009) *Aspergillus fumigatus* Conidial Melanin Modulates Host Cytokine Response. *Immunobiology*.
11. Pihet M, Vandeputte P, Tronchin G, Renier G, Saulnier P, et al. (2009) Melanin is an essential component for the integrity of the cell wall of *Aspergillus fumigatus* conidia. *BMC Microbiol* 9: 177.
12. Youngchim S, Morris-Jones R, Hay RJ, Hamilton AJ (2004) Production of melanin by *Aspergillus fumigatus*. *J Med Microbiol* 53: 175-181.
13. Aimanianda V, Bayry J, Bozza S, Knemeyer O, Perruccio K, et al. (2009) Surface hydrophobin prevents immune recognition of airborne fungal spores. *Nature* 460: 1117-1121.
14. Paris S, Debeaupuis JP, Cramer R, Carey M, Charles F, et al. (2003) Conidial hydrophobins of *Aspergillus fumigatus*. *Appl Environ Microbiol* 69: 1581-1588.
15. Thau N, Monod M, Crestani B, Rolland C, Tronchin G, et al. (1994) rodletless mutants of *Aspergillus fumigatus*. *Infect Immun* 62: 4380-4388.

Early Development *A. fumigatus* proteome profile

16. Gautam P, Sundaram CS, Madan T, Gade WN, Shah A, et al. (2007) Identification of novel allergens of *Aspergillus fumigatus* using immunoproteomics approach. *Clin Exp Allergy* 37: 1239-1249.
17. Gravelat FN, Doedt T, Chiang LY, Liu H, Filler SG, et al. (2008) In vivo analysis of *Aspergillus fumigatus* developmental gene expression determined by real-time reverse transcription-PCR. *Infect Immun* 76: 3632-3639.
18. Teutschbein J, Albrecht D, Potsch M, Guthke R, Amanianda V, et al. (2010) Proteome profiling and functional classification of intracellular proteins from conidia of the human-pathogenic mold *Aspergillus fumigatus*. *J Proteome Res* 9: 3427-3442.
19. Beranova-Giorgianni S (2003) Proteome analysis by two-dimensional gel electrophoresis and mass spectrometry: strengths and limitations. *Trac-Trends in Analytical Chemistry* 22: 273-+.
20. Ross PL, Huang YN, Marchese JN, Williamson B, Parker K, et al. (2004) Multiplexed protein quantitation in *Saccharomyces cerevisiae* using amine-reactive isobaric tagging reagents. *Mol Cell Proteomics* 3: 1154-1169.
21. Zieske LR (2006) A perspective on the use of iTRAQ reagent technology for protein complex and profiling studies. *J Exp Bot* 57: 1501-1508.
22. Cagas SE, Jain MR, Li H, Perlin DS (2011) Profiling the *Aspergillus fumigatus* proteome in response to caspofungin. *Antimicrob Agents Chemother* 55: 146-154.
23. Niki Y, Bernard EM, Edwards FF, Schmitt HJ, Yu B, et al. (1991) Model of recurrent pulmonary aspergillosis in rats. *J Clin Microbiol* 29: 1317-1322.

Early Development *A. fumigatus* proteome profile

24. Saeed AI, Sharov V, White J, Li J, Liang W, et al. (2003) TM4: a free, open-source system for microarray data management and analysis. *Biotechniques* 34: 374-378.
25. Hosack DA, Dennis G, Jr., Sherman BT, Lane HC, Lempicki RA (2003) Identifying biological themes within lists of genes with EASE. *Genome Biol* 4: R70.
26. McDonagh A, Fedorova ND, Crabtree J, Yu Y, Kim S, et al. (2008) Sub-telomere directed gene expression during initiation of invasive aspergillosis. *PLoS Pathog* 4: e1000154.
27. Jain MR, Bian S, Liu T, Hu J, Elkabes S, et al. (2009) Altered proteolytic events in experimental autoimmune encephalomyelitis discovered by iTRAQ shotgun proteomics analysis of spinal cord. *Proteome Sci* 7: 25.
28. Keller A, Nesvizhskii AI, Kolker E, Aebersold R (2002) Empirical statistical model to estimate the accuracy of peptide identifications made by MS/MS and database search. *Anal Chem* 74: 5383-5392.
29. Kall L, Storey JD, MacCoss MJ, Noble WS (2008) Assigning significance to peptides identified by tandem mass spectrometry using decoy databases. *J Proteome Res* 7: 29-34.
30. Nesvizhskii AI, Keller A, Kolker E, Aebersold R (2003) A statistical model for identifying proteins by tandem mass spectrometry. *Anal Chem* 75: 4646-4658.
31. Taubitz A, Bauer B, Heesemann J, Ebel F (2007) Role of respiration in the germination process of the pathogenic mold *Aspergillus fumigatus*. *Curr Microbiol* 54: 354-360.

Early Development *A. fumigatus* proteome profile

32. Woo PC, Chong KT, Lau CC, Wong SS, Lau SK, et al. (2006) A novel approach for screening immunogenic proteins in *Penicillium marneffe* using the DeltaAFMP1DeltaAFMP2 deletion mutant of *Aspergillus fumigatus*. *FEMS Microbiol Lett* 262: 138-147.

Table 1: All Proteins Identified by iTRAQ and Protein Fold Changes

UniProt ID	Molecular Weight	ORF Name	Gene Name	Common Name of Target	4 HOURS	8 HOURS	16 HOURS	Unique Peptides	% Coverage
Q4WKG5	50 kDa	AFUA_8G00630		Putative uncharacterized protein	-24.8	-15.8	-17.2	2	6%
Q4WJZ0	23 kDa	AFUA_5G09240	sodC	Superoxide dismutase [Cu-Zn]	-18.8	-19.4	-6.2	4	23%
Q4WK69	32 kDa	AFUA_5G09580	rodA	Hydrophobin	-10.6	-18.4	-10.9	3	11%
Q4WKL3	35 kDa	AFUA_2G17530	abr2	Brown 2	-10.2	-25.2	-24.3	3	12%
Q4WK23	119 kDa	AFUA_3G14540		Heat shock protein Hsp30/Hsp42, putative	-9.5	-28.6	-10.6	2	2%
Q4WK03	81 kDa	AFUA_4G08240		Zinc-containing alcohol dehydrogenase, putative	-4.2	-12.4	-6.2	7	11%
Q4WJR3	33 kDa	AFUA_4G13120		Glutamine synthetase	-3.2	-3.5	-2.9	3	8%
Q4WK14	21 kDa	AFUA_4G07710		Pyruvate carboxylase, putative	-2.8	-6.8	-7.0	4	27%
Q4WP12	23 kDa	AFUA_5G09230		Transaldolase	-2.6	-2.7	-1.4	2	12%
Q4X1C0	16 kDa	AFUA_1G11480		Putative uncharacterized protein	-2.5	-2.1	-1.3	3	17%
Q4WLK1	14 kDa	AFUA_3G11070	pdca	Pyruvate decarboxylase	-2.5	-6.8	1.7	5	28%
Q4WIE8	55 kDa	AFUA_6G06750		14-3-3 family protein	-2.3	-2.8	-1.5	7	17%
Q4WJN2	33 kDa	AFUA_3G14490		Ketol-acid reductoisomerase	-2.0	-2.3	-2.5	2	8%
Q4WJW9	17 kDa	AFUA_5G02910		NAP family protein	-2.0	-2.8	-4.2	2	10%
Q4WJQ1	120 kDa	AFUA_6G01940		Dienelactone hydrolase family protein	-2.0	-5.2	-2.8	3	4%
Q4WJN7	25 kDa	AFUA_6G06770	enoA	Enolase	-1.9	-3.1	-2.6	4	15%
Q4WJH1	23 kDa	AFUA_5G13450		Triosephosphate isomerase	-1.8	-2.9	-2.3	5	19%
Q4X0L0	26 kDa	AFUA_3G08380		Inorganic diphosphatase, putative	-1.8	-1.8	-1.2	3	14%
Q6MYW4	24 kDa	AFUA_3G11690		Fructose-bisphosphate aldolase, class II	-1.8	-2.0	-1.7	6	29%
Q4WAI8	28 kDa	AFUA_4G03410		Flavohemoprotein	-1.8	-3.3	1.7	6	23%
Q4WYW9	20 kDa	AFUA_7G05740		Malate dehydrogenase	-1.8	-0.7	0.0	5	23%
Q4WY39	40 kDa	AFUA_3G07430	asp f 27	Cyclophilin	-1.8	-1.9	-0.5	5	17%
Q6MY48	22 kDa	AFUA_1G11190		Eukaryotic translation elongation factor 1 subunit Eef1-beta,	-1.8	-1.4	-1.5	5	24%

				putative					
Q4WTV5	37 kDa	AFUA_6G04920		NAD-dependent formate dehydrogenase AciA/Fdh	-1.8	-3.1	1.2	3	11%
Q4WCP3	35 kDa	AFUA_1G04620		Alcohol dehydrogenase, zinc-containing, putative	-1.7	-2.2	1.3	2	6%
Q4WC88	60 kDa	AFUA_3G06460		Putative uncharacterized protein	-1.7	1.4	2.5	9	19%
P61832	15 kDa	AFUA_7G00250		Tubulin beta chain	-1.7	-2.1	-1.6	3	16%
Q4WIE3	13 kDa	AFUA_8G01670	katG	Catalase-peroxidase	-1.7	-2.9	-1.4	2	14%
Q4X1I3	32 kDa	AFUA_5G10780		UDP-glucose 4-epimerase	-1.6	-3.0	-1.3	3	10%
Q4WGP3	36 kDa	AFUA_5G14680		Putative uncharacterized protein	-1.6	-2.9	2.1	6	29%
Q4WLN1	86 kDa	AFUA_2G03720	cpr2	Peptidyl-prolyl cis-trans isomerase B	-1.6	-0.8	1.6	8	12%
Q4WDF5	54 kDa	AFUA_5G06240		Alcohol dehydrogenase, putative	-1.6	-1.8	1.3	8	18%
Q4WLM5	29 kDa	AFUA_1G10350		Phosphoglycerate kinase	-1.6	-1.4	1.7	10	39%
Q4WT91	48 kDa	AFUA_1G05080		60S ribosomal protein P0	-1.6	-1.4	-1.9	6	17%
Q4WJR7	45 kDa	AFUA_2G10070		Carbamoyl-phosphate synthase, large subunit	-1.6	-2.3	-2.9	3	12%
Q4WCM2	67 kDa	AFUA_8G05600		Putative uncharacterized protein	-1.6	-1.9	2.5	4	7%
Q4WNZ0	19 kDa	AFUA_6G02280	pmp20	Putative peroxiredoxin pmp20	-1.6	-2.2	0.4	3	14%
Q4WP16	65 kDa	AFUA_6G04740		Actin Act1	-1.6	-1.5	1.1	2	5%
Q4WJV9	38 kDa	AFUA_5G06680		4-aminobutyrate transaminase GatA	-1.5	-2.7	-3.8	2	8%
Q4WWF0	17 kDa	AFUA_3G04220		Fatty acid synthase beta subunit, putative	-1.5	-1.8	-1.2	3	18%
Q4WZS4	48 kDa	AFUA_2G16090		Karyopherin alpha subunit, putative	-1.5	-1.1	-1.2	2	11%
Q4WEU5	52 kDa	AFUA_5G02450		Farnesyl-pyrophosphate synthetase	-1.4	-1.2	1.2	6	16%
Q4WXW 4	37 kDa	AFUA_4G11550		Putative uncharacterized protein	-1.4	0.1	-0.7	11	32%
Q4WEB8	40 kDa	AFUA_5G08830		Woronin body protein HexA, putative	-1.4	-1.8	1.2	3	8%
Q4WQK8	35 kDa	AFUA_1G14200		Mitochondrial processing peptidase beta subunit, putative	-1.4	-1.3	1.1	8	21%
Q6MYM6	45 kDa	AFUA_8G03930		Hsp70 chaperone (HscA),	-1.4	-1.5	-1.7	2	9%

				putative					
P41746	16 kDa	AFUA_7G05720		Pyruvate dehydrogenase complex, dihydrolipoamide acetyltransferase component, putative	-1.4	1.1	1.3	2	19%
Q4WTJ3	22 kDa	AFUA_5G06390		Adenosine kinase, putative	-1.4	-2.3	-2.0	6	30%
Q4WYD9	60 kDa	AFUA_2G03720		Peptidyl-prolyl cis-trans isomerase	-1.4	-1.7	-0.4	3	4%
Q4WMB9	27 kDa	AFUA_2G11060		Acyl CoA binding protein family	-1.4	-2.1	1.5	3	17%
Q4WJD7	21 kDa	AFUA_6G11620		Formyltetrahydrofolate deformylase, putative	-1.4	-2.2	-2.3	5	30%
Q4WJ94	13 kDa	AFUA_6G08050		6-phosphogluconate dehydrogenase, decarboxylating	-1.3	-2.5	-2.2	2	8%
Q4X205	12 kDa	AFUA_2G06150		Protein disulfide isomerase Pdi1, putative	-1.3	-3.0	-1.3	4	21%
Q4WZM7	53 kDa	AFUA_2G10030		Actin cytoskeleton protein (VIP1), putative	-1.3	-4.0	-1.2	2	5%
Q4WLQ2	9 kDa	AFUA_2G03010		Cytochrome c subunit Vb, putative	-1.3	0.0	1.6	3	23%
Q4WT53	23 kDa	AFUA_2G09790		Glucose-6-phosphate isomerase	-1.3	-2.3	-1.9	5	12%
Q873W8	16 kDa	AFUA_1G09440	rps23	40S ribosomal protein S23	-1.3	-1.7	-2.0	4	23%
Q4WHU8	20 kDa	AFUA_6G05210		Malate dehydrogenase, NAD-dependent	-1.3	-2.3	-1.4	6	36%
Q4WWC7	48 kDa	AFUA_1G13490		Spermidine synthase	-1.3	-1.2	-1.2	4	15%
Q4WP13	72 kDa	AFUA_2G13010		Cytochrome c oxidase polypeptide vib	-1.3	-1.7	1.1	4	6%
Q4WWX5	18 kDa	AFUA_1G03510		ATP synthase gamma chain	-1.3	-1.7	-1.1	6	39%
Q4WV25	56 kDa	AFUA_4G07580		Translation initiation factor EF-2 gamma subunit, putative	-1.2	1.4	1.3	13	32%
Q4WE70	36 kDa	AFUA_6G03810		ATP synthase D chain, mitochondrial, putative	-1.2	-1.1	1.1	5	14%
Q4WI29	29 kDa	AFUA_1G10630		S-adenosylmethionine synthetase	-1.2	1.2	1.4	3	13%

Q4WSG1	35 kDa	AFUA_5G07120		RNP domain protein	-1.2	-1.4	-1.7	8	36%
Q4WYL7	35 kDa	AFUA_8G05320		ATP synthase subunit alpha	-1.2	-1.2	-0.4	2	3%
Q4WSY6	25 kDa	AFUA_1G13500		Transketolase TktA	-1.2	-2.0	-1.7	8	45%
Q4WRN1	15 kDa	AFUA_4G07360		Cobalamin-independent methionine synthase Meth/D	-1.2	-2.2	-1.5	2	16%
Q4WMV5	53 kDa	AFUA_5G01970		Glyceraldehyde 3-phosphate dehydrogenase	-1.1	-1.2	1.5	2	6%
Q4WP20	20 kDa	AFUA_5G10550		ATP synthase subunit beta	-1.1	-1.2	1.1	4	16%
Q4WGP1	52 kDa	AFUA_4G12450		57 kDa immunogenic protein	-1.1	-1.2	2.1	3	13%
Q6MY77	57 kDa	AFUA_4G13700		Threonyl-tRNA synthetase, putative	-1.1	-1.4	-1.5	3	7%
Q4WX01	58 kDa	AFUA_4G13170		G-protein complex beta subunit CpcB	-1.1	1.1	-1.1	2	4%
Q7Z7W6	84 kDa	AFUA_6G07720		Phosphoenolpyruvate carboxykinase AcuF	-1.0	-2.3	2.4	2	3%
Q4WVGJ9	17 kDa	AFUA_6G03820	egd2	Nascent polypeptide-associated complex subunit alpha	-0.8	2.1	1.9	3	20%
Q4WZH8	10 kDa	AFUA_1G05390		Mitochondrial ADP,ATP carrier protein (Ant), putative	-0.8	0.6	-1.2	4	48%
Q9C177	23 kDa	AFUA_6G07770		Alanine aminotransferase, putative	-0.7	-1.6	1.4	2	12%
Q4X0D4 (+1)	16 kDa	AFUA_3G05600		60S ribosomal protein L27a, putative	-0.7	1.2	-1.2	3	23%
Q4WND4	30 kDa	AFUA_2G15940		Cofactor for methionyl-and glutamyl-tRNA synthetases, putative	-0.7	-1.6	-1.4	4	14%
Q4WTP5	16 kDa	AFUA_2G02100		Dihydrolipoyl dehydrogenase	-0.7	-0.4	1.2	4	25%
Q4WT69	45 kDa	AFUA_6G12930		Mitochondrial aconitate hydratase, putative	-0.6	-1.9	-1.9	7	21%
Q4WN34	55 kDa	AFUA_3G05370		Dihydrolipoamide succinyltransferase, putative	-0.6	-1.1	1.5	6	13%
Q4WYA0	13 kDa	AFUA_5G03490	ndk1	Nucleoside diphosphate kinase	-0.6	-1.3	-0.4	2	18%
Q4WWC 5	15 kDa	AFUA_2G13860		Histone H4	-0.6	0.6	-1.2	6	34%
Q8TGG6	48 kDa	AFUA_4G09140		L-ornithine aminotransferase	-0.6	-1.7	-1.7	5	15%

				Car2, putative					
Q4WJK8	29 kDa	AFUA_1G05500		40S ribosomal protein S12	-0.6	-1.8	-2.3	7	29%
Q4X0M1	11 kDa	AFUA_1G02070		Cytochrome C1/Cyt1, putative	-0.6	-1.3	-1.2	4	45%
Q4WSZ2	22 kDa	AFUA_2G04310		Argininosuccinate synthase	-0.5	-1.6	-1.8	8	38%
Q9Y8D9	16 kDa	AFUA_6G04570		Translation elongation factor eEF-1 subunit gamma, putative	-0.5	1.5	1.3	2	21%
Q4WT41	42 kDa	AFUA_1G13710		Isoleucyl-tRNA synthetase, cytoplasmic	-0.4	-1.9	-1.8	6	17%
Q6MYM4	80 kDa	AFUA_2G16400		Translation initiation factor 4B	-0.4	-1.3	-1.7	8	12%
Q4WX86	31 kDa	AFUA_1G10130		Adenosylhomocysteinase	-0.4	-1.2	-1.1	2	8%
Q4X1G1	18 kDa	AFUA_5G07300		Electron transfer flavoprotein, beta subunit, putative	-0.4	-1.6	-1.3	2	10%
Q4X1E0	24 kDa	AFUA_6G02470		Fumarate hydratase, putative	-0.2	-1.9	-1.3	5	34%
Q4WI99	62 kDa	AFUA_1G06960		Pyruvate dehydrogenase E1 component alpha subunit, putative	-0.2	-1.5	-1.4	2	7%
Q4WHT0	46 kDa	AFUA_6G13550		Ribosomal protein S13p/S18e	-0.1	-0.6	-1.4	2	5%
Q4WEH4	41 kDa	AFUA_6G10660		ATP citrate lyase subunit (Acl), putative	-0.1	-1.4	1.2	10	32%
Q4WNH3	50 kDa	AFUA_5G10560		Cytochrome c oxidase subunit V	-0.1	-1.4	1.4	7	17%
Q4WRU9	26 kDa	AFUA_5G04160		NTF2 and RRM domain protein	-0.1	-1.5	-1.5	5	21%
Q4WAQ6	15 kDa	AFUA_3G08770		NADH-ubiquinone oxidoreductase subunit GRIM-19, putative	-0.1	1.3	1.7	8	41%
Q4X1P9	11 kDa	AFUA_4G11050		NADH-ubiquinone oxidoreductase, subunit F, putative	-0.1	-1.4	-1.3	2	11%
Q4WTW7	27 kDa	AFUA_6G10650		ATP citrate lyase, subunit 1, putative	-0.1	-1.4	1.2	6	28%
Q4WTX0	37 kDa	AFUA_1G12170		Elongation factor Tu	-0.1	0.4	1.2	3	11%
Q4WYW4	56 kDa	AFUA_5G06130		Succinyl-CoA synthetase alpha subunit, putative	0.0	-0.2	-0.1	2	4%
Q4W9L9	26 kDa	AFUA_3G07640		Plasma membrane H ⁺ -ATPase Pma1	0.0	-1.6	0.0	9	37%
Q4WP18	131 kDa	AFUA_1G07440		Molecular chaperone Hsp70	0.0	1.5	1.1	2	3%

Q4WXX9	63 kDa	AFUA_3G13320	rps0	40S ribosomal protein S0	0.0	1.3	-0.7	3	7%
Q4WRF2	10 kDa	AFUA_6G06370		NAD(+)-isocitrate dehydrogenase subunit I	0.0	-1.5	-1.5	5	29%
Q8TF79	122 kDa	AFUA_8G03880		Alanyl-tRNA synthetase, putative	0.0	-1.8	-1.6	3	3%
Q876M7	90 kDa	AFUA_6G05200		60S ribosomal protein L28	0.0	1.2	-1.2	3	5%
Q4WJ75	41 kDa	AFUA_5G07020		Ribosome biogenesis ABC transporter Arb1, putative	0.0	-1.2	-2.2	2	5%
Q4WYK1	32 kDa	AFUA_4G09870		Putative uncharacterized protein	0.0	-1.6	-0.4	5	20%
Q4WQR1	84 kDa	AFUA_5G04170	hsp90	Heat shock protein 90	0.0	1.7	1.1	3	5%
Q4WUL0	61 kDa	AFUA_2G02590		Aspartyl-tRNA synthetase Dps1, putative	0.0	1.6	1.2	2	4%
Q4WA70 (+1)	50 kDa	AFUA_2G08130		60S ribosomal protein L44	0.0	2.2	1.7	2	6%
Q4WGN6	118 kDa	AFUA_2G10090		40S ribosomal protein S15, putative	0.0	2.6	1.9	7	8%
Q4WZR7	71 kDa	AFUA_3G09320		Serine hydroxymethyltransferase	0.0	-1.3	-1.2	2	5%
Q4WH99	56 kDa	AFUA_2G03290		14-3-3 family protein ArtA, putative	0.0	-1.6	-1.3	3	7%
Q4WU60	28 kDa	AFUA_1G04070		Eukaryotic translation initiation factor eIF-5A	0.0	2.1	1.2	2	10%
Q4WMU1	38 kDa	AFUA_1G11130		60S ribosomal protein L6	0.0	2.0	1.5	2	9%
Q4WC61	9 kDa	AFUA_2G13110		Cytochrome c	0.0	1.7	2.6	3	39%
Q4WI57	22 kDa	AFUA_4G11650		Alpha-ketoglutarate dehydrogenase complex subunit Kgd1, putative	0.0	-1.5	-1.4	4	35%
Q4WTN7	48 kDa	AFUA_1G11710		Ribosomal protein L1	0.0	1.5	1.2	2	5%
Q4WEE8	18 kDa	AFUA_6G02520		Eukaryotic translation initiation factor eIF-1A subunit, putative	0.0	1.4	1.2	4	23%
Q4WUP8	35 kDa	AFUA_6G06900		GTPase Rho1	0.1	-1.3	1.2	4	16%
Q4WQD6	57 kDa	AFUA_2G16820		Curved DNA-binding protein (42 kDa protein)	0.1	1.3	1.1	12	23%
Q4WHY9	22 kDa	AFUA_2G16010		Prolyl-tRNA synthetase	0.1	-1.4	-1.4	2	11%
Q4X1J1	61 kDa	AFUA_1G12590		La protein homolog, putative	0.1	1.6	-1.3	2	3%

Q4WLH1	15 kDa	AFUA_5G02750		Cytochrome c oxidase subunit Va, putative	0.1	0.4	1.7	4	24%
Q4WW75	25 kDa	AFUA_6G10450		Putative uncharacterized protein	0.2	-3.7	1.3	6	33%
Q4WRB8	20 kDa	AFUA_2G10500		40S ribosomal protein Rps16, putative	0.3	-1.3	-1.5	4	23%
Q4WN06	56 kDa	AFUA_3G11260		Ubiquitin (UbiC), putative	0.3	1.4	1.5	3	6%
Q4WPG1	49 kDa	AFUA_1G06390		Elongation factor 1-alpha	0.4	1.3	1.1	3	9%
Q4WP70	37 kDa	AFUA_1G04320		Ribosomal protein S8	0.4	1.3	1.1	2	7%
Q4WWR1	18 kDa	AFUA_1G12610	hsp88	Heat shock protein Hsp88, putative	0.4	1.1	-1.1	3	15%
Q4WD82	16 kDa	AFUA_5G04230		Citrate synthase	0.4	1.1	1.3	3	24%
Q4WZI4	47 kDa	AFUA_1G04530		Ribosomal L18ae protein family	0.4	1.3	-1.2	4	12%
Q4X220	25 kDa	AFUA_3G08600		Translational initiation factor 2 beta	0.4	-1.2	-1.3	4	18%
Q4X1P8	26 kDa	AFUA_3G12690		Putative uncharacterized protein	0.4	-1.5	-1.3	7	30%
Q4WWZ4	109 kDa	AFUA_1G09100		60S ribosomal protein L9, putative	0.4	1.3	-1.1	3	4%
Q6MY67	33 kDa	AFUA_1G03970		Mitochondrial translation initiation factor IF-2, putative	0.5	-1.2	-1.5	4	10%
Q4WDM0	35 kDa	AFUA_3G05350	htb1	Histone H2B	0.5	1.7	1.4	2	10%
Q4WWT2	27 kDa	AFUA_3G06970		40S ribosomal protein S9	0.6	1.2	-1.1	4	20%
Q9UVW1	65 kDa	AFUA_1G05040		Protein mitochondrial targeting protein (Mas1), putative	0.6	-0.6	-1.2	2	4%
Q4WSV7	20 kDa	AFUA_2G10010		Nonsense-mediated mRNA decay protein (Nmd5), putative	0.6	-1.2	-1.7	2	9%
Q4WM42	30 kDa	AFUA_2G07380		Ribosomal protein L18	0.8	2.3	1.6	4	10%
Q4WZQ9	61 kDa	AFUA_6G03830		Ribosomal protein L14	0.8	-1.2	-1.2	3	6%
Q4WEX7	205 kDa	AFUA_1G02550		Tubulin alpha-1 subunit	0.8	-1.5	-1.2	6	3%
Q4WJV5	28 kDa	AFUA_3G07710		Nucleolin protein Nsr1, putative	1.0	0.8	-3.0	4	19%
Q4WEV9	73 kDa	AFUA_5G03020		60S ribosomal protein L4, putative	1.1	1.5	1.2	2	4%
Q4WXF4	52 kDa	AFUA_3G06840		40S ribosomal protein S4, putative	1.1	1.3	-1.1	6	15%
Q4WP49	70 kDa	AFUA_1G04190	pab1	Polyadenylate-binding protein,	1.1	1.9	1.1	2	5%

				cytoplasmic and nuclear					
Q4WD81	22 kDa	AFUA_2G07970		60S ribosomal protein L19	1.1	1.6	1.3	3	21%
Q8NKF4	44 kDa	AFUA_2G04130		40S ribosomal protein S11	1.1	-0.4	-1.3	14	35%
Q4X1G7	28 kDa	AFUA_5G06360		60S ribosomal protein L8, putative	1.1	-1.1	-1.3	2	8%
Q4WWT1	18 kDa	AFUA_2G16370		60S ribosomal protein L32	1.1	1.2	-1.1	4	28%
Q4WJD2	54 kDa	AFUA_7G05660		Translation elongation factor eEF-3, putative	1.1	0.4	-2.2	16	41%
Q4WJ30	70 kDa	AFUA_4G07660	ded1	ATP-dependent RNA helicase ded1	1.1	-1.7	-2.1	19	30%
Q4X1G9	119 kDa	AFUA_1G05200	tif32	Eukaryotic translation initiation factor 3 subunit A	1.2	1.2	-1.3	2	2%
Q4WWN 1	16 kDa	AFUA_3G08160	tif1	ATP-dependent RNA helicase eIF4A	1.2	1.1	-1.2	3	31%
Q4WP05	56 kDa	AFUA_2G10300		40S ribosomal protein S17, putative	1.2	1.3	0.6	2	5%
Q4WV26	22 kDa	AFUA_1G13790	hhtA	Histone H3	1.2	1.3	1.3	4	23%
Q4WI54	21 kDa	AFUA_6G07430		Pyruvate kinase	1.2	-1.2	-1.4	3	14%
Q4WU42	37 kDa	AFUA_1G16523		40S ribosomal protein S25, putative	1.2	1.4	1.2	4	16%
Q4WX09	71 kDa	AFUA_5G05630		60S ribosomal protein L23	1.2	1.2	-1.1	4	8%
Q4X0G7	93 kDa	AFUA_1G10510		60S ribosomal protein L35	1.2	1.2	-1.2	17	23%
Q4X279	21 kDa	AFUA_2G09870	tif35	Eukaryotic translation initiation factor 3 subunit G	1.2	-1.1	-1.3	2	11%
Q4WB08	37 kDa	AFUA_7G04210		Tropomyosin, putative	1.2	0.6	2.2	2	6%
Q4WCV0	21 kDa	AFUA_4G06910		Outer mitochondrial membrane protein porin	1.2	-1.5	1.3	2	15%
Q4WXA2	15 kDa	AFUA_2G09960		Mitochondrial Hsp70 chaperone (Ssc70), putative	1.2	1.1	-1.1	2	21%
Q6MYD1	33 kDa	AFUA_3G01110	gua1	GMP synthase [glutamine- hydrolyzing]	1.2	-1.1	-1.6	3	10%
Q4WCX4	21 kDa	AFUA_1G12890		60S ribosomal protein L5, putative	1.2	1.8	1.3	4	20%
Q4WZN0	15 kDa	AFUA_7G02140		40S ribosomal protein S24	1.2	1.2	-1.2	4	30%
Q4WM07	32 kDa	AFUA_6G12720		40S ribosomal protein S29,	1.2	2.0	1.6	3	13%

				putative					
Q4WD80	29 kDa	AFUA_1G16840		Translationally-controlled tumor protein homolog	1.2	1.3	1.3	6	31%
Q4WCU6	63 kDa	AFUA_3G12300		60S ribosomal protein L22, putative	1.2	1.6	1.3	4	7%
Q4WFT3	61 kDa	AFUA_1G05630		40S ribosomal protein S3, putative	1.3	1.2	-1.2	4	7%
Q4WQK3	40 kDa	AFUA_4G03860	nip1	Eukaryotic translation initiation factor 3 subunit C	1.3	2.1	1.1	3	8%
Q4WVI1	28 kDa	AFUA_3G10920		Telomere and ribosome associated protein Stm1, putative	1.3	1.6	1.3	3	15%
Q4WXZ8	18 kDa	AFUA_1G15020		40S ribosomal protein S5, putative	1.3	1.3	-0.6	6	36%
Q4W9S8	98 kDa	AFUA_2G09210		60S ribosomal protein L10	1.3	1.3	0.0	2	4%
Q4WWR9	29 kDa	AFUA_1G06340		60S ribosomal protein L27	1.3	1.3	-1.1	9	33%
Q4WX65	44 kDa	AFUA_2G13530		Translation elongation factor EF-2 subunit, putative	1.3	1.2	-1.1	7	18%
Q4WX73	13 kDa	AFUA_1G06770		40S ribosomal protein S26	1.3	1.1	-1.1	2	6%
Q4WVV5	28 kDa	AFUA_2G03040		Ribosomal protein L34 protein, putative	1.3	1.9	1.3	3	14%
Q4X1M0	164 kDa	AFUA_2G11850	rpl3	60S ribosomal protein L3	1.3	-1.1	-1.3	3	2%
Q4W9U9	51 kDa	AFUA_1G15730		40S ribosomal protein S22	1.3	1.2	0.0	2	6%
P40292	81 kDa	AFUA_3G04210		Fatty acid synthase alpha subunit FasA	1.3	-1.2	1.2	15	19%
Q4W9S6	34 kDa	AFUA_5G05540		Nucleosome assembly protein Nap1, putative	1.3	-1.1	0.0	7	24%
Q4WDJ0	46 kDa	AFUA_4G07730		60S ribosomal protein L11	1.3	1.9	1.3	7	19%
Q7Z8P9	17 kDa	AFUA_6G13250		60S ribosomal protein L31e	1.3	1.5	1.2	4	36%
Q4WX43	46 kDa	AFUA_7G01460		Ribosomal protein S5	1.3	1.2	-1.1	7	19%
Q4WN39	67 kDa	AFUA_6G12660		40S ribosomal protein S10b	1.4	2.1	1.5	2	5%
Q4WDH2	44 kDa	AFUA_3G06960		60S ribosomal protein L21, putative	1.4	1.8	1.3	5	16%
Q4WNT7	37 kDa	AFUA_4G08030		Putative uncharacterized protein	1.4	1.2	0.1	5	16%

Q4X1G3	129 kDa	AFUA_2G17110	25d9-4	Cdc48p	1.4	-1.4	-1.3	3	4%
Q4WSA0	75 kDa	AFUA_4G03650		Ribosome associated DnaJ chaperone Zuotin, putative	1.4	-1.2	-1.6	9	13%
Q4WEX6	232 kDa	AFUA_2G09490		Eukaryotic translation initiation factor subunit eIF-4F, putative	1.4	1.1	-1.2	6	4%
Q4WNT6	72 kDa	AFUA_1G14410	rpl17	60S ribosomal protein L17	1.4	1.4	0.0	2	2%
Q4WQ57	119 kDa	AFUA_2G09200		60S ribosomal protein L30, putative	1.4	1.4	1.1	8	11%
Q4WEG3	41 kDa	AFUA_3G13480		Translation initiation factor 2 alpha subunit, putative	1.4	1.4	1.2	2	4%
Q4WET8	57 kDa	AFUA_1G04660		Ribosomal protein L15	1.4	1.8	1.2	2	4%
Q4WTU5	35 kDa	AFUA_3G10730		40S ribosomal protein S7e	1.4	1.6	1.2	4	15%
Q4WDL9	17 kDa	AFUA_3G07810		Succinate dehydrogenase subunit Sdh1, putative	1.4	-1.1	1.3	3	15%
Q4WM99	79 kDa	AFUA_6G02750	egd1	Nascent polypeptide-associated complex subunit beta	1.4	1.8	1.5	9	13%
Q4WQ47	34 kDa	AFUA_4G03880		60S ribosomal protein L7	1.5	1.7	1.1	2	7%
Q4WPX5	27 kDa	AFUA_5G04370		NADH-ubiquinone oxidoreductase, subunit G, putative	1.5	-1.1	1.1	5	19%
Q4WCU3	18 kDa	AFUA_1G14120		Nuclear segregation protein (Bfr1), putative	1.5	1.8	1.3	3	17%
Q4WJ44	47 kDa	AFUA_4G06900		Asparagine synthetase Asn2, putative	1.5	-1.4	-2.1	4	10%
Q4X1H5	74 kDa	AFUA_6G08720		5'-methylthioadenosine phosphorylase (Meu1), putative	1.5	1.2	-1.3	8	13%
Q4WLQ8	18 kDa	AFUA_6G02440		60S ribosomal protein L24a	1.5	2.2	1.6	3	10%
Q4WPN3	14 kDa	AFUA_4G04460		60S ribosomal protein L13	1.5	1.5	1.1	2	8%
Q4WG92	18 kDa	AFUA_3G06760		Ribosomal protein L37	1.5	2.2	1.8	2	14%
Q4WV46	41 kDa	AFUA_2G08670		Acetyl-CoA carboxylase	1.5	1.2	1.3	2	8%
Q4WNY2	87 kDa	AFUA_4G07435		60S ribosomal protein L36	1.6	1.4	0.4	8	13%
Q4WTM9	29 kDa	AFUA_6G12990		Cytosolic large ribosomal subunit protein L7A	1.6	1.6	1.2	7	35%
Q4WS30	53 kDa	AFUA_1G14220		Fibrillarin	1.6	1.2	-1.5	4	12%

Q4WM98	53 kDa	AFUA_2G16880		60S ribosomal protein L37a	1.7	2.0	1.5	7	18%
Q4X164	17 kDa	AFUA_1G07280		Putative uncharacterized protein	1.7	-1.1	-1.3	4	29%
Q4WU32	70 kDa	AFUA_3G08460		60S ribosomal protein L35Ae	1.7	1.8	1.2	2	6%
Q4WN66	58 kDa	AFUA_4G10800		40S ribosomal protein S6	1.7	2.1	1.4	5	9%
O43099	18 kDa	AFUA_7G05290		40S ribosomal protein S13	1.7	1.8	1.3	5	27%
Q96X30	47 kDa	AFUA_2G02150		40S ribosomal protein S10a	1.8	2.0	1.4	11	32%
Q4WXU5	23 kDa	AFUA_6G11260		Ribosomal protein L26	1.8	1.2	-1.1	8	34%
Q6J9U0	77 kDa	AFUA_5G05450	rps1	40S ribosomal protein S1	1.9	2.0	1.4	2	4%
Q4WPZ9	55 kDa	AFUA_1G05990		Ribosomal protein L16a	1.9	1.5	1.1	3	5%
Q4W9X3	46 kDa	AFUA_1G05340		40S ribosomal protein S19	1.9	0.6	0.0	3	10%
Q4WJM1	16 kDa	AFUA_6G08580	fpr4	FK506-binding protein 4	1.9	2.1	-2.4	3	20%
Q4WCM7	114 kDa	AFUA_5G12180		<i>Ran-specific GTPase-activating protein 1, putative</i>	2.1	2.1	2.5	2	2%
Q4X1V2	255 kDa	AFUA_6G06340		Glucosamine-fructose-6-phosphate aminotransferase	2.2	-1.5	-1.3	2	1%
Q4WTZ9	55 kDa	AFUA_4G07690		Phosphoribosylaminoimidazolecarboxamide formyltransferase/IMP cyclohydrolase	2.3	0.4	1.2	2	5%

Proteins in italics change 2-fold or greater at all 3 time points

Table 2: Genes with Largest Changes at 8 and 16 Hours and GO Terms Associated with Gene Changes

8 Hours Microarray Data							
ORF Name	Common Name of Target	Average Fold Change					
AFUA_8G04550	ComA domain protein	-153.7					
AFUA_5G01160	monosaccharide transporter	-120.9					
AFUA_6G12000	hypothetical protein	-120.4					
AFUA_7G01010	alcohol dehydrogenase, putative	-103.3					
AFUA_8G02440	c-4 methyl sterol oxidase	29.6					
AFUA_5G08830	HEX1	34.2					
16 Hours Microarray Data							
AFUA_4G13510	isocitrate lyase	-172.8					
AFUA_1G01490	hypothetical protein	-158.5					
AFUA_5G10050	cytochrome P450 monooxygenase, putative	-150.8					
AFUA_5G01160	monosaccharide transporter	-142.0					
AFUA_6G12000	hypothetical protein	-135.5					
AFUA_5G10070	dehydrogenase	-115.5					
AFUA_4G09600	GPI anchored protein, putative	-114.8					
AFUA_7G01010	alcohol dehydrogenase, putative	-107.8					
AFUA_2G03830	allergen Asp F4	89.2					
AFUA_2G09030	secreted dipeptidyl peptidase	93.4					
AFUA_2G11520	MFS monosaccharide transporter, putative	98.5					
AFUA_4G01290	endo-chitosanase, pseudogene	115.3					
File	Term	List Hits	List Size	Pop. Hits	Pop. Size	Fisher's Exact	
8 Hour							
GO Biological Process	fatty acid beta-oxidation	9	453	15	4696	1.98E-06	Decreasing

GO Biological Process	fatty acid catabolic process	7	453	14	4696	1.40E-04	Decreasing
GO Biological Process	autophagy	7	453	17	4696	6.11E-04	Decreasing
GO Biological Process	hyperosmotic response	3	453	3	4696	8.92E-04	Decreasing
GO Cellular Component	peroxisomal matrix	12	412	30	4148	1.29E-05	Decreasing
GO Cellular Component	integral to peroxisomal membrane	4	412	4	4148	9.61E-05	Decreasing
GO Molecular Function	zinc ion binding	43	470	219	4823	4.04E-06	Decreasing
GO Molecular Function	specific RNA polymerase II transcription factor activity	7	470	17	4823	6.51E-04	Decreasing
GO Molecular Function	two-component sensor activity	6	470	13	4823	7.84E-04	Decreasing
GO Biological Process	translation	107	718	149	4696	2.50E-56	Increasing
GO Cellular Component	cytosolic large ribosomal subunit (sensu Eukaryota)	42	689	45	4148	5.33E-30	Increasing
GO Cellular Component	cytosolic small ribosomal subunit (sensu Eukaryota)	28	689	35	4148	1.93E-16	Increasing
GO Molecular Function	structural constituent of ribosome	96	711	118	4823	9.53E-61	Increasing
	16 Hour						
GO Biological Process	fatty acid beta-oxidation	8	237	15	4696	1.77E-07	Decreasing
GO Biological Process	N-acetylglucosamine catabolic process	4	237	5	4696	3.04E-05	Decreasing
GO Cellular Component	peroxisomal matrix	10	219	30	4148	1.62E-06	Decreasing
GO Cellular Component	peroxisome	6	219	23	4148	9.56E-04	Decreasing
GO Molecular Function	electron transporter activity	4	249	10	4823	1.14E-03	Decreasing
GO Biological Process	translation	88	590	149	4696	4.78E-43	Increasing
GO Cellular Component	cytosolic large ribosomal subunit (sensu Eukaryota)	42	563	45	4148	9.14E-34	Increasing
GO Cellular Component	cytosolic small ribosomal subunit (sensu Eukaryota)	29	563	35	4148	2.71E-20	Increasing
GO Molecular Function	structural constituent of ribosome	81	591	118	4823	8.01E-48	Increasing

Table 3: Comparison of Protein vs. Gene Expression Values at 8 Hours (2-fold or Greater)

UniProt ID	ORF Name	Gene Name	Common Name of Target	Molecular Weight	Average 8 Hour Protein Fold Change	Average 8 Hour Gene Fold Change
Q4WYW9	AFUA_3G14540		Heat shock protein Hsp30/Hsp42, putative	20 kDa	-28.6	-25.5
Q9UVW1	AFUA_2G17530	abr2	Brown 2	65 kDa	-25.2	NI
Q9Y8D9	AFUA_5G09240	sodC	Superoxide dismutase [Cu-Zn]	16 kDa	-19.4	NI
P41746	AFUA_5G09580	rodA	Hydrophobin	16 kDa	-18.4	NI
Q4WB08	AFUA_8G00630		Putative uncharacterized protein	37 kDa	-15.8	NI
Q4WP70	AFUA_4G08240		Zinc-containing alcohol dehydrogenase, putative	37 kDa	-12.4	-2.3
Q4WXX9	AFUA_3G11070	pdca	Pyruvate decarboxylase	63 kDa	-6.8	NI
Q4WP18	AFUA_4G07710		Pyruvate carboxylase, putative	131 kDa	-6.8	2.5
Q4WCP3	AFUA_6G01940		Dienelactone hydrolase family protein	35 kDa	-5.2	-2.7
Q4X1G7	AFUA_2G10030		Actin cytoskeleton protein (VIP1), putative	28 kDa	-4.0	NI
Q4WMB9	AFUA_6G10450		Putative uncharacterized protein	27 kDa	-3.7	NI
Q4WQK3	AFUA_4G13120		Glutamine synthetase	40 kDa	-3.5	-20.6
Q4W9X3	AFUA_4G03410		Flavohepotein	46 kDa	-3.3	14.2
Q4WDJ0	AFUA_6G04920		NAD-dependent formate dehydrogenase AciA/Fdh	46 kDa	-3.1	NI
Q96X30	AFUA_6G06770	enoA	Enolase	47 kDa	-3.1	6.7
Q4WV46	AFUA_5G10780		UDP-glucose 4-epimerase	41 kDa	-3.0	2.6
Q4WH99	AFUA_2G06150		Protein disulfide isomerase Pdi1, putative	56 kDa	-3.0	3.0
Q4WW75	AFUA_5G14680		Putative uncharacterized protein	25 kDa	-2.9	NI
Q7Z7W6	AFUA_8G01670	katG	Catalase-peroxidase	84 kDa	-2.9	-2.0
Q4WVV5	AFUA_5G13450		Triosephosphate isomerase	28 kDa	-2.9	3.8
Q4WEG3	AFUA_5G02910		NAP family protein	41 kDa	-2.8	NI
Q4WI29	AFUA_6G06750		14-3-3 family protein	29 kDa	-2.8	3.5
Q4WUP8	AFUA_5G09230		Transaldolase	35 kDa	-2.7	NI
Q4WTZ9	AFUA_5G06680		4-aminobutyrate transaminase	55 kDa	-2.7	6.0

			GatA			
Q4WN06	AFUA_6G08050		6-phosphogluconate dehydrogenase, decarboxylating	56 kDa	-2.5	2.1
Q4X1J1	AFUA_2G09790		Glucose-6-phosphate isomerase	61 kDa	-2.3	3.5
Q4WDM0	AFUA_6G05210		Malate dehydrogenase, NAD-dependent	35 kDa	-2.3	2.1
Q4X1G3	AFUA_2G10070		Carbamoyl-phosphate synthase, large subunit	129 kDa	-2.3	4.5
Q4WN39	AFUA_6G07720		Phosphoenolpyruvate carboxykinase AcuF	67 kDa	-2.3	-2.8
Q4WTX0	AFUA_5G06390		Adenosine kinase, putative	37 kDa	-2.3	5.1
Q4WYW4	AFUA_3G14490		Ketol-acid reductoisomerase	56 kDa	-2.3	NI
Q4WJV9	AFUA_1G04620		Alcohol dehydrogenase, zinc-containing, putative	38 kDa	-2.2	2.4
Q4WM07	AFUA_6G11620		Formyltetrahydrofolate deformylase, putative	32 kDa	-2.2	2.7
Q4WNY2	AFUA_4G07360		Cobalamin-independent methionine synthase MetH/D	87 kDa	-2.2	3.5
O43099	AFUA_6G02280	pmp20	Putative peroxiredoxin pmp20	18 kDa	-2.2	9.3
Q4X164	AFUA_2G11060		Acyl CoA binding protein family	17 kDa	-2.1	4.8
Q4WSV7	AFUA_1G11480		Putative uncharacterized protein	20 kDa	-2.1	3.3
Q4WA70 (+1)	AFUA_7G00250		Tubulin beta chain	50 kDa	-2.1	NI
Q4WSA0	AFUA_1G13500		Transketolase TktA	75 kDa	-2.0	3.3
Q4WY39	AFUA_3G11690		Fructose-bisphosphate aldolase, class II	40 kDa	-2.0	3.0
Q4WLQ2	AFUA_6G12720		40S ribosomal protein S29, putative	9 kDa	2.0	9.2
Q4WSZ2	AFUA_1G11130		60S ribosomal protein L6	22 kDa	2.0	6.3
Q4WTM9	AFUA_5G05450	rps1	40S ribosomal protein S1	29 kDa	2.0	8.5
Q4WIE3	AFUA_2G02150		40S ribosomal protein S10a	13 kDa	2.0	9.5
Q4WZH8	AFUA_2G16880		60S ribosomal protein L37a	10 kDa	2.0	11.2
Q4WMV5	AFUA_6G08580	fpr4	FK506-binding protein 4	53 kDa	2.1	NI
Q4W9S8	AFUA_4G03860	nip1	Eukaryotic translation initiation factor 3 subunit C	98 kDa	2.1	3.0

Q4WD81	AFUA_6G03820	egd2	Nascent polypeptide-associated complex subunit alpha	22 kDa	2.1	15.3
Q4WK14	AFUA_1G04070		Eukaryotic translation initiation factor eIF-5A	21 kDa	2.1	5.9
Q4WLQ8	AFUA_6G12660		40S ribosomal protein S10b	18 kDa	2.1	9.2
Q4WV11	AFUA_5G12180		Ran-specific GTPase-activating protein 1, putative	28 kDa	2.1	4.6
Q4WPX5	AFUA_4G10800		40S ribosomal protein S6	27 kDa	2.1	9.6
Q4WCU3	AFUA_6G02440		60S ribosomal protein L24a	18 kDa	2.2	12.5
Q4WWR1	AFUA_3G06760		Ribosomal protein L37	18 kDa	2.2	6.2
Q4X205	AFUA_2G08130		60S ribosomal protein L44	12 kDa	2.2	10.6
Q4X279	AFUA_2G07380		Ribosomal protein L18	21 kDa	2.3	7.5
Q4X1G1	AFUA_2G10090		40S ribosomal protein S15, putative	18 kDa	2.6	8.3

NI-Not Identified

Table 4: Comparison of Protein vs. Gene Expression Values at 16 Hours (2-fold or Greater)

UniProt ID	ORF Name	Gene Name	Common Name of Target	Molecular Weight	Average 16 Hour Protein Fold Change	Average 16 Hour Gene Fold Change
Q9UVW1	AFUA_2G17530	abr2	Brown 2	65 kDa	-24.3	NI
Q4WB08	AFUA_8G00630		Putative uncharacterized protein	37 kDa	-17.2	NI
P41746	AFUA_5G09580	rodA	Hydrophobin	16 kDa	-10.9	NI
Q4WYW9	AFUA_3G14540		Heat shock protein Hsp30/Hsp42, putative	20 kDa	-10.6	NI
Q4WP18	AFUA_4G07710		Pyruvate carboxylase, putative	131 kDa	-7.0	NI
Q9Y8D9	AFUA_5G09240	sodC	Superoxide dismutase [Cu-Zn]	16 kDa	-6.2	NI
Q4WP70	AFUA_4G08240		Zinc-containing alcohol dehydrogenase, putative	37 kDa	-6.2	NI
Q4WEG3	AFUA_5G02910		NAP family protein	41 kDa	-4.2	NI
Q4WTZ9	AFUA_5G06680		4-aminobutyrate transaminase GatA	55 kDa	-3.8	NI
Q4WX01	AFUA_3G07710		Nucleolin protein Nsr1, putative	58 kDa	-3.0	-2.8
Q4X1G3	AFUA_2G10070		Carbamoyl-phosphate synthase, large subunit	129 kDa	-2.9	NI
Q4WQK3	AFUA_4G13120		Glutamine synthetase	40 kDa	-2.9	-20.9
Q4WCP3	AFUA_6G01940		Dienelactone hydrolase family protein	35 kDa	-2.8	2.8
Q96X30	AFUA_6G06770	enoA	Enolase	47 kDa	-2.6	5.7
Q4WYW4	AFUA_3G14490		Ketol-acid reductoisomerase	56 kDa	-2.5	NI
Q4WMV5	AFUA_6G08580	fpr4	FK506-binding protein 4	53 kDa	-2.4	NI
Q4WJM1	AFUA_1G05500		40S ribosomal protein S12	16 kDa	-2.3	6.8
Q4WVV5	AFUA_5G13450		Triosephosphate isomerase	28 kDa	-2.3	3.4
Q4WM07	AFUA_6G11620		Formyltetrahydrofolate deformylase, putative	32 kDa	-2.3	NI
Q4WGN6	AFUA_7G05660		Translation elongation factor eEF-3, putative	118 kDa	-2.2	-12.5
Q4WN06	AFUA_6G08050		6-phosphogluconate dehydrogenase, decarboxylating	56 kDa	-2.2	NI
Q4WU32	AFUA_5G07020		Ribosome biogenesis ABC transporter Arb1, putative	70 kDa	-2.2	-4.7
Q4WNT6	AFUA_4G06900		Asparagine synthetase Asn2, putative	72 kDa	-2.1	-2.2

Q4WP13	AFUA_4G07660	ded1	ATP-dependent RNA helicase ded1	72 kDa	-2.1	-8.4
Q4WTX0	AFUA_5G06390		Adenosine kinase, putative	37 kDa	-2.0	6.7
Q873W8	AFUA_1G09440	rps23	40S ribosomal protein S23	16 kDa	-2.0	5.9
Q4WW75	AFUA_5G14680		Putative uncharacterized protein	25 kDa	2.1	24.3
Q4WQD6	AFUA_4G12450		57 kDa immunogenic protein	57 kDa	2.1	5.7
Q4WG92	AFUA_7G04210		Tropomyosin, putative	18 kDa	2.2	11.5
Q4WN39	AFUA_6G07720		Phosphoenolpyruvate carboxykinase AcuF	67 kDa	2.4	-7.6
Q4WV11	AFUA_5G12180		Ran-specific GTPase-activating protein 1, putative	28 kDa	2.5	4.2
Q4WC61	AFUA_8G05600		Putative uncharacterized protein	9 kDa	2.5	32.9
Q4WWN1	AFUA_3G06460		Putative uncharacterized protein	16 kDa	2.5	8.9
Q4X0L0	AFUA_2G13110		Cytochrome c	26 kDa	2.6	NI

NI- Not Identified

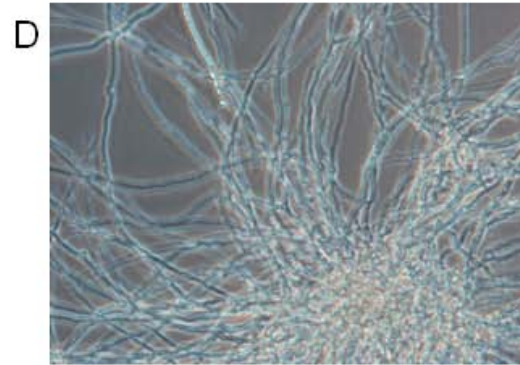
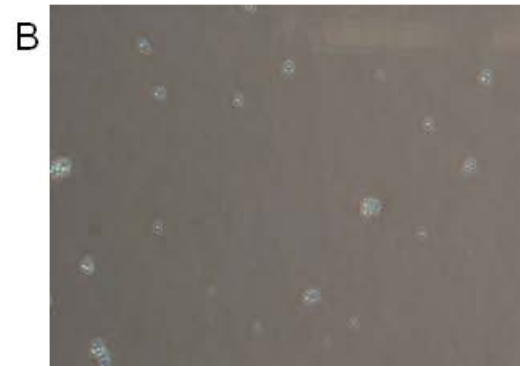
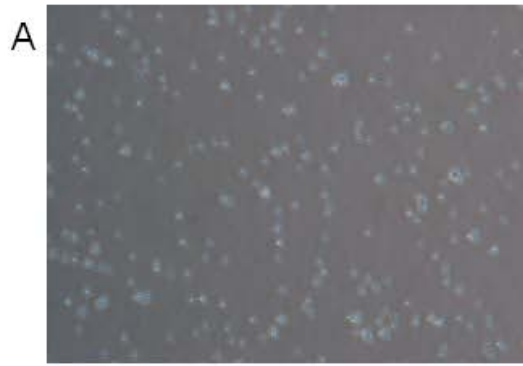


Figure 1

Figure Legends

Figure 1: *Aspergillus fumigatus* early growth morphology. 40X microscopic images of *Aspergillus fumigatus* strain R21 taken at (A) 0 hours, (B) 4 hours in which the conidia are beginning to aggregate and swell, (C) 8 hours at which germ tubes are beginning to form, and (D) 16 hours when full mature mycelia are visible.